Full-field strain measurements of the inside of an agricultural tyre using digital image correlation

Filip Feldesi, Theunis R. Botha* and P. Schalk Els

University of Pretoria, South Africa

*Corresponding author.
E-mail addresses: u13015673@tuks.co.za (F. Feldesi),
theunis.botha@up.ac.za (T.R. Botha),
schalk.els@up.ac.za (P.S. Els).

Highlights

- The strain inside an agricultural tyre with large lugs has a very non-homogeneous strain pattern.
- Possible to measure strain on the inside of a tyre using digital image correlation.
- Linear relationships between strain and vertical force are obtained at different of inflation pressure.
- Linear relationship between the longitudinal force and strain were obtained.

Abstract

This paper investigates strain measured on the inside of an agricultural tyre with large tread-blocks during a series of static tests using a novel measuring system. The full field strain measurements may be used in the development of a tyre which is capable of estimating tyre forces from strain measurements. The strain measurement system makes use of a calibrated stereo camera system on a mechanical stabilizing system that keeps the cameras pointed at the inside surface of the tyre in contact with the road while the wheel rotates. A static tyre test rig is used to displace the road surface relative to the tyre in the vertical and longitudinal direction. The large tread-blocks caused strain concentrations on the inner surface as the tyre deforms to comply with the road surface. Vertical and longitudinal tests each produce unique strain patterns in the contact patch region. Relationships between the applied forces and strain measurements were developed and showed that these relationships are near linear with R^2 values above 0.97. The strain measurements also show that the location where strain gauges, for single point strain measurements, are placed inside the tyre is very important on large lugged tyres.

Keywords

Contact patch
Stereovision
Strain
Tread-block
Digital image correlation

1. Introduction

The tyre-terrain interface is one of the most important regions of terramechanics and vehicle research as the majority of forces between the vehicle and the environment are generated at this interface. Recently a large body of research has been performed on the development of a tyre which can estimate the states of the tyre such as tyre inflation pressure and vertical load. With most studies focusing on single point measurements, using strain gauges, to determine tyre states. Strain gauges are mainly used due to their simplicity of use and low cost solution to measuring strain. Tuononen, 2008, Tuononen, 2009 used a single LED, glued to the inside of the tyre, and a two-dimensional position sensitive detector to measure the position of the LED from which the deflection of the tyre was determined. From the deflection measurements, estimates of the lateral tyre force were made. Niskanen and Tuononen (2014) used 3 tri-axial accelerometers to study the tyre-terrain contact on wet surfaces and showed that the system can determine the onset of vehicle aquaplaning Braghin et al. (2006) also used accelerometer measurement on the inside of the tyre to determine the tyre sideslip angle and the vertical tyre force. Hong et al. (2013) made use of an accelerometer to determine the friction coefficient of the tyre terrain interface based on estimating the deflection of the tyre. Garcia-Pozuelo et al. (2017) used strain gauge measurement to study the relationship between strain, vertical load and inflation pressure. Their work found that it would be possible to use strain measurements to determine the vertical load on the tyre. Garcia-Pozuelo, et al. (2019) used Kyowa's KFEL series of high-elongation, 10–15% strain, foil strain gauges on the inside tyre surface to measure strain in a small slick tyre for SAE Formula Student. The strain measurements were used to validate a mathematical tyre model. The maximum strain measured on the inside of the tyre, during normal operating conditions, was around 3%. No study investigating the strain on the inside of an agricultural tyre could be found, however it is expected that agricultural tyres will have larger strains compared to the SAE Formula Student tyres due to differences in construction and inflation pressure. Therefore high-elongation strain gauges are required to measure the strain inside the tyre. The use of newer conductive thermoplastic elastomers have made it possible to measure very high strains up to 400% (Fan et al., 2012). Ruggeri and Vecchiattini (2018) developed a conductive thermoplastic elastomer (CTPE) sensor to measure strain in the contact patch region. The sensor has a similar stiffness to the tyre and therefore does not affect the tyre behaviour or performance. Three sensors measure strain in three directions over three select lines, measuring the average strain, but can be adapted to produce measurements over many locations to potentially produce full field measurements. The geometry of the sensor and material can be varied to suit the application. Ruggeri and Vecchiattini (2018) use the longitudinal sensor to measure longitudinal strain in a tyre as it is rolled over a flat surface and as it is rolled onto a small step. While Ruggeri and Vecchiattini (2018) have managed to measure strains in the contact patch region, the sensors are in the early stages of testing and would need to be tested for repeatability and sensitivity to operating conditions. While strain guages that can measure very high strains do exists, they are only capable of measuring the strain at a single point, they are therefore, illsuited to measure full-field strain.

Optical sensors have been used in previous studies to measure the tyre radial deflection and was shown to provide information on the vertical load (Tuononen, 2011) Studies have also shown that the radial deflection can be used to provide information on both the vertical and longitudinal forces. This is due to the coupling of the deformation in the radial and tangential directions, with a tangential deformation resulting in radial deformation and vice versa. Thus, by only measuring the radial deformation it could be possible to estimate both the vertical and longitudinal forces on the tyre (Xiong and Tuononen, 2015). The use of cameras to study the inside of a tyre has been used in previous studies. Hiroaka et al. (2009) first proposed using a camera inside the tyre to capture the inner tyre surface to measure in-plane strain. Hiroaka used a single camera mounted to the rim pointing at the tyre surface. The single viewpoint meant that it was not able to determine the out of plane strain and could not account for apparent strain when the tyre deflects closer to the camera. Green (2011) acknowledged the need to account for out of plane effects and attempted to use a single viewpoint to capture the inner surface of the tyre while attempting to recover the out of plane deflection from the amount of image blur created by the out of plane motion. Green was not able to recover the depth and only improved on the accuracy of Hiroaka by using a finer sub-pixel interpolation scheme. Guthrie et al. (2017) used a calibrated stereo camera system to measure the 3D profile of the inside of a tyre while driving over objects. While successful Guthrie et al. (2017) makes no inference on the tyre deformation or strain. Most of the studies also perform measurements on road tyres with almost no work performed on agricultural tyres with large lugs.

In this study the works of Guthrie et al., 2017, Green, 2011 are combined by using a stereo vision based measurement system to measure the plane strain on the inside of the tyre while accounting for the out of plane motion. The study also performs the measurements on a large lugged agricultural tyre as currently no such study exists in literature, as all current studies make use of passenger tyres with relatively smooth tread. The final aim of this study is to provide information on the strain field of an agricultural tyre which can be used to locate ideal position to place single point strain gauges with the aim to develop an agricultural tyre from which tyre states can be estimated. In particular the study aims to determine whether the large lugs of an agricultural tyre has a significant effect on the strain developed on the inside of the tyre during loading.

2. Material and methods

In this study a calibrated stereo camera setup is used along with a digital image correlation algorithm to measure the strain on the inside of the tyre. Tests are conducted on a static test rig to apply different loading conditions to the tyre. The strain measurement system and test rig are discussed in more detail in the following sections

2.1. Strain measurement system

A special Tyre-Terrain Camera (T2Cam) system was developed which allows a pair of calibrated stereo cameras to always view the area of the tyre in contact with the terrain from the inside of the tyre(Guthrie et al. 2017). The T2Cam system makes use of two sets of planetary gears; one on the inside of a vehicle wheel and an identical one on the outside, with the same gear ratio, as shown in Fig. 1 (a). The planetary gears are connected by shafts with seals to maintain tyre inflation pressure. By keeping the outside sun gear stationary, the inside sun gear remains stationary while the wheel rotates. The cameras and data acquisition system are mounted to the inner sun gear and remain stationary, with the cameras constantly pointing at the region in contact with the terrain. Power to the system is provided by means of a slip ring assembly. The data acquisition system makes use of two high speed Pointgrey Flea3 (FL3-U3-13Y3M-C) cameras with Kowa LMN4NCL wide angle lenses to capture the entire region in contact with the terrain. The cameras are connected to a MintBox Mini single chip computer that stores the data on board and then transmits it wirelessly to an external computer for post processing using the inverse computation Gauss-Newton digital image correlation algorithm (Botha et al. 2017), (Baker & Mattews, 2004). Changes made to the setup used by Guthrie et al. (2017) was to move from a narrow camera baseline (distance between cameras) to a wider baseline to improve accuracy, as shown in Fig. 1(b) (Feldesi et al. 2018). The cameras had a baseline of 347 mm with a 60° angle relative to one another and therefore a 30° angle relative to a vertical line. The cameras were mounted on a radius of about 250 mm from the centre of the tyre.

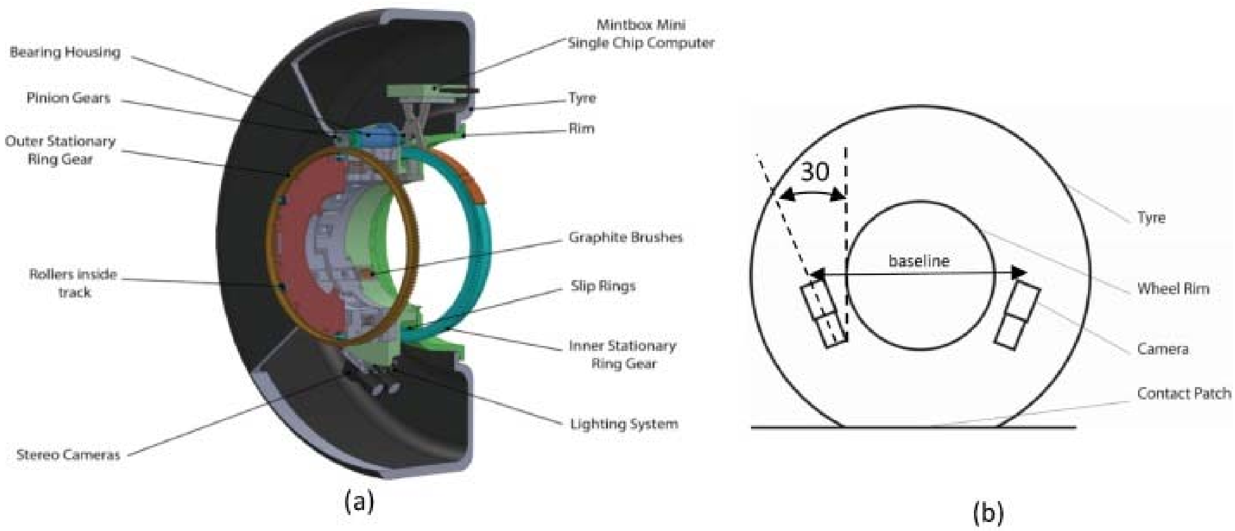

Fig. 1. (a) T2Cam system used to measure strain inside the tyre (Guthrie et al. 2017), (b) Side view showing location of cameras mounted inside the wheel.

The strain is determined from the displacement field between the two different states. Thus, to obtain the strain field, the displacement field needs to be determined first. The displacement field is determined by finding the position of points, relative to the camera, in two different states. The position of the points in a state is determined using digital image correlation which maps a region in the left camera image to the right camera image, of the same state, in sub-pixel accuracy by optimising a correlations function. The 2D mapping, in pixels, is transformed into a 3D mapping using triangulation as well as the known orientation and translation between cameras and the lens intrinsic parameters. All the required information are obtained during calibration (Feldesi et al. 2018). By determining the position in two states, the difference in position can be determined which produces a deformation field. The first state is a reference state assumed to be un-deformed and the second state is the current deformed state. It should be noted that the reference state need not be an un-deformed state. The deformation and strain is assumed to be zero at the reference state and therefore deformation and strain is measured relative to this state. In terms of a tyre the reference state can be an uninflated tyre, inflated tyre or even a vertically loaded tyre and the strain is then measured relative to these states. Fig. 2 shows sample images for a reference state (inflated un-deformed tyre) and for the current deformed state (a vertically loaded tyre). The strain is determined using a Constant Strain Triangle (CST) element which is fitted to neighbouring deformation points. For each point, four triangles are used and the strain is taken as the average of these four triangles. This allows the plane longitudinal, lateral and shear strains to be calculated at a specific location.

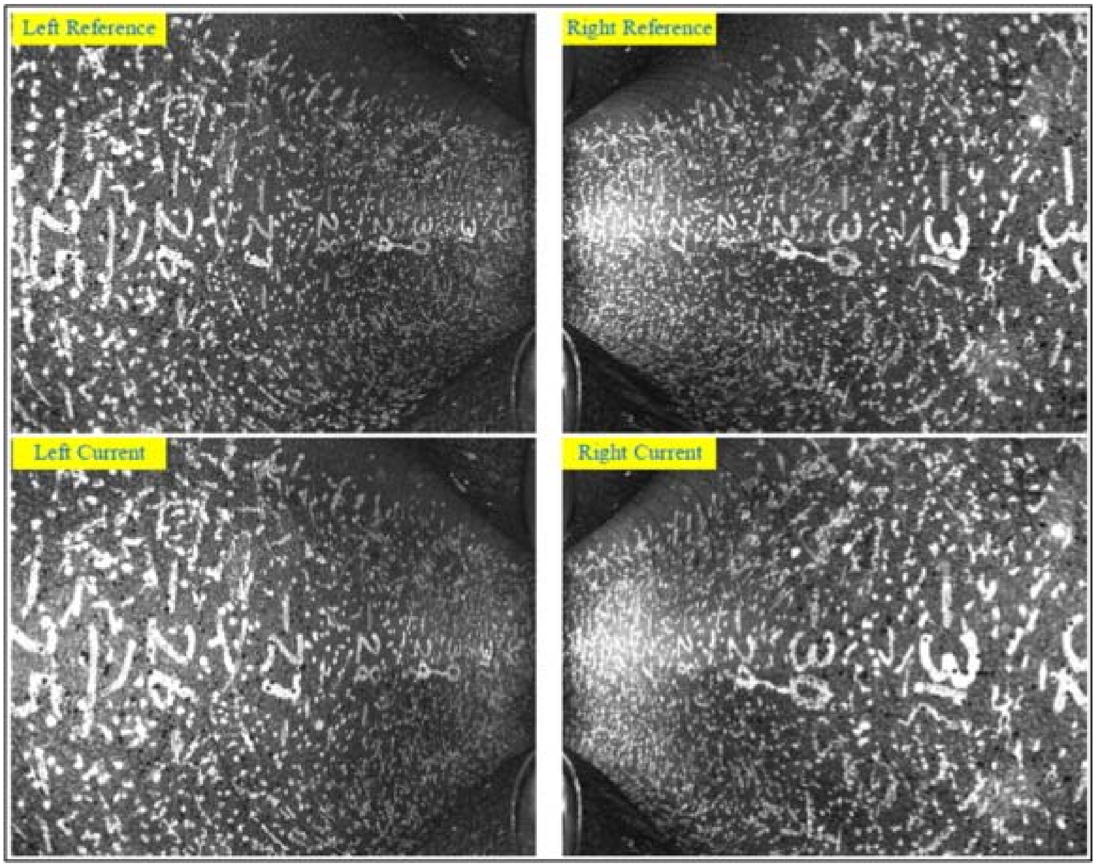

Fig. 2. Sample images for a reference and deformed (current) state.

2.2. Tyre test setup

The T2Cam strain measurement system is mounted on the inside of the tyre on a special rim. The rim is mounted to an in house developed Wheel Force Transducer (WFT) to measure the forces and moment in the three principle directions (longitudinal, lateral and vertical) at the centre of the wheel. The entire wheel is mounted on a static tyre test rig, shown in Fig. 3 (a, c). The static test rig allows the road surface, in contact with the tyre, to be actuated in the three principle directions. Therefore, the tyre can be initially vertically loaded after which either a lateral or longitudinal load can be applied to the tyre. Currently the static test rig is in displacement control using a bang-bang or on–off controller. Therefore, the displacement or applied forces cannot be accurately controlled however all forces on the tyre are measured using the WFT. The agricultural tyre, a 16-inch Trelleborg TM700 280/70R16 TL 112A8 (112B) with orchards/vineyards tread pattern, used for this test has large tread-blocks as shown in Fig. 3 (b). It is expected that the large lugs will have a significant effect on the strain measurements on the inside of the tyre.

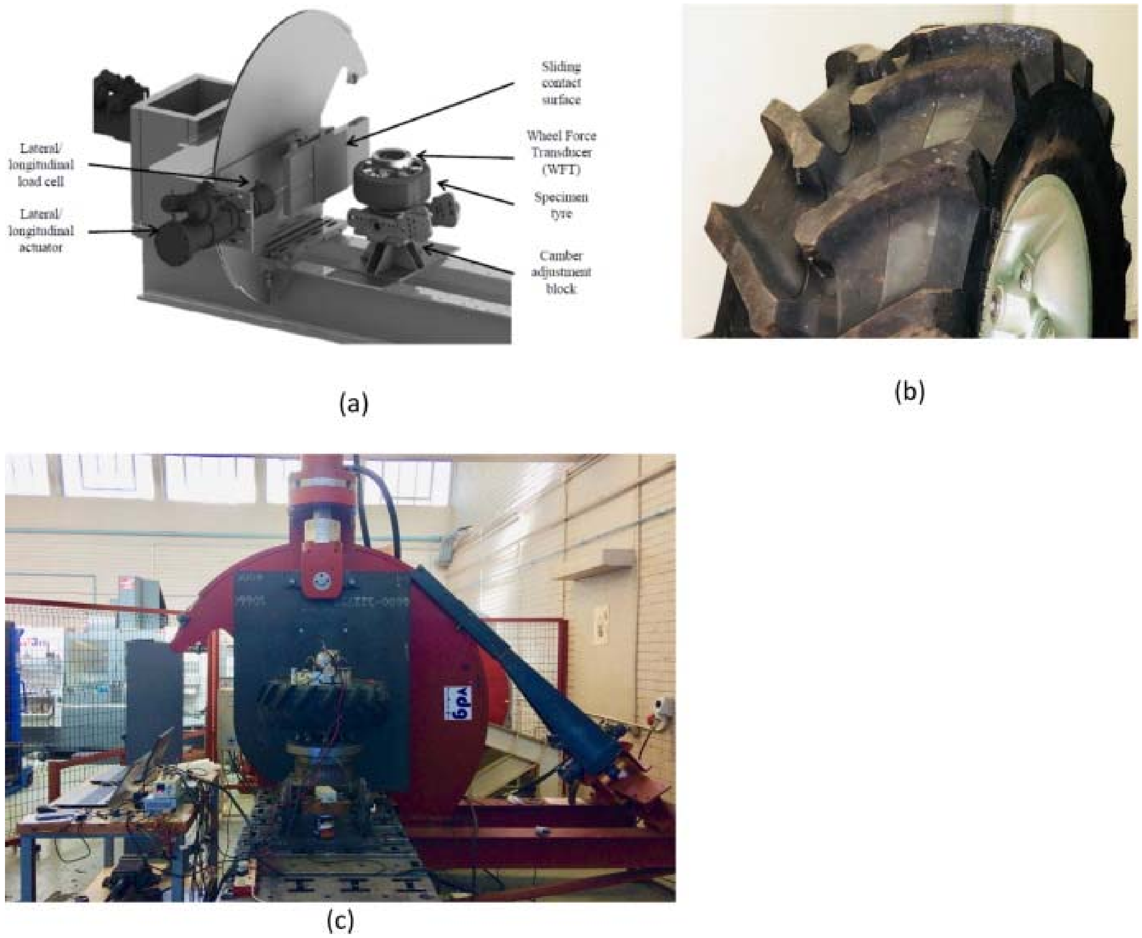

Fig. 3. a) Static tyre test rig used to apply loads to the tyre b) Test tyre a 16 in. agricultural Tyre from Trelleborg c) Test tyre on static test rig.

2.3. Testing procedure

The internal measurement system of the T2Cam was synchronised with the external data acquisition system, which measured the forces using the WFT and displacements, by conducting quasi-static tests. During the tests the tyre obtained a static state at which images were taken using the T2Cam and measurements were taken using the external data acquisition system. Tests were performed in a slow incremental manner taking samples at each displacement increment. The quasi-static nature of the tests also ensures that there are no thermal effects. To determine whether the large lugs of the tyre have an effect on the strain pattern three different statically loaded tests were performed. The three tests performed on the static test rig are:

- Inflation Test
- Vertical Load Test
- Longitudinal Load Test

The test procedure for each test was as follows.

2.3.1. Inflation test procedure

The inflation test was performed by mounting the tyre on the static test rig completely deflated. Reference images of the tyre deflated to 0 kPa were taken using T2Cam. The tyre was inflated in stages with increments of 40 kPa. At each inflation pressure, images of the inside of the tyre was taken to determine the strain relative to the uninflated tyre. In the test, the tyre is inflated from 0 kPa to about 300 kPa, thus having measurements at inflation pressures of 0, 40, 80, …, 300Kpa.

2.3.2. Vertical load test procedure

Different vertical loads are applied on the tyre while taking force and strain measurements. Initially reference images of the inside of the unloaded and inflated tyre are taken with T2Cam. The vertical load is then incrementally increased from 0 N in steps of 500 N until the maximum load, which is dependent on the inflation pressure, is reached as specified by the manufacturer. Once a specific load is reached the load is held constant while the average forces are measured and images of the inside of the tyre are taken using T2Cam. Since the actuator does not have very fine control, the applied vertical loads may vary slightly, approximately 150 N variation, from test to test.

The test was conducted at three different tyre inflation pressures, 160, 200 and 240 kPa in order to determine the effect tyre inflation pressure has on the strain measurement. The maximum vertical load for each pressure was based on the load index of the tyre given as 8.5kN, 10kN, and 11kN for tyre inflation pressures of 160, 200 and 240 kPa respectively. was The inflation pressure is measured prior to each test using a certified digital pressure gauge. The inflation pressure is also recorded on the external data acquisition system using a pressure sensor. At each inflation pressure a different maximum applied force, as specified by the manufacturer, is applied.

2.3.3. Longitudinal load test procedure

In the longitudinal test the tyre is first vertically loaded to a desired vertical load. Reference images of the inside of the tyre are taken of the inflated vertically unloaded and inflated vertically loaded tyre. The tyre is then incrementally loaded longitudinally by displacing the tyre in the longitudinal direction in steps. At specific longitudinal displacements the load and longitudinal displacement on the tyre is held constant and images of the inside of the tyre are captured along with force and displacement measurements. The displacement is measured using an Acuity AR700 road profiling laser, with 200 mm range and 50 µm measurement resolution. The longitudinal displacement is increased until slippage occurs between the tread and road surface. The road surface is first displaced to the left until the tyre slips after which it is displaced to the right, without removing the vertical load, until the tyre slips. It should be noted that the load application represents how the tyre would be loaded on hard terrain as in soft terrain the lugs will be embedded in the soil. This will result in different loads being applied to the lugs as the soil is sheared in between lugs. This may affect the strain measurements and should be further investigated in future studies.

3. Results and discussion

3.1. Tyre inflation pressure effect

The effect of any external loading on the contact patch strain remains largely unknown. An inflation test has no external loading and creates an evenly distributed loading on the inside of the tyre. Therefore, on a tyre where the tread is more homogeneous the results should be similar to a pressure vessel resulting in a uniform strain distribution. The strain is calculated relative to an 0 kPa tyre inflation pressure with the weight of the tyre acting laterally down, thus the tyre is not in a completely un-deformed state. The strain in an area the size of the contact patch, at the highest inflation pressure, 29 kPa, is shown in Fig. 4. A visual observation reveals that, as expected, the strain is non-uniform and that the strain varies near the tread blocks as the blocks increase the tread stiffness. The strain pattern does however appear repetitive in both lateral and longitudinal direction as the tyre construction is non-homogenous but repetitive along the circumference. Thus, one expects to see a repeated strain pattern along the circumference as the loading on the tyre is uniform everywhere. A two-dimensional line segment is extracted from the contact patch to reveal localised strain information. A line along the circumference between 64 mm and 66 mm laterally is chosen, illustrated in black on Fig. 4. This section has three segments of repeating strain pattern due to the three lugs. The data contains some noise which affects the ability to distinguish global peaks and troughs. The raw data is smoothed, using a five-point moving average filter in MATLAB. The raw and smoothed strain of the section is plotted against longitudinal distance in Fig. 5. The peaks were obtained when the smoothed curve reached a maximum within a 10 mm window. Using the detected peaks, indicated by stars, and neglecting the first peak which is close to the edge and subject to edge effects in the algorithm the second, third and fourth peak have very similar longitudinal strain, and all lie within a 0.1% strain band of one another. This partially validates the strain measurement in the central region of the contact patch region, as the system was able to capture a repeating trend due to the uniform pressure loading. The results also indicate that the lugs significantly affect the tyre stiffness in the circumferential directions. As mentioned a uniform stiffness pressure vessel would have the same strain along the circumference. The peaks observed in Fig. 5, indicate large strain changes and thus change in stiffness around the tyre circumference.

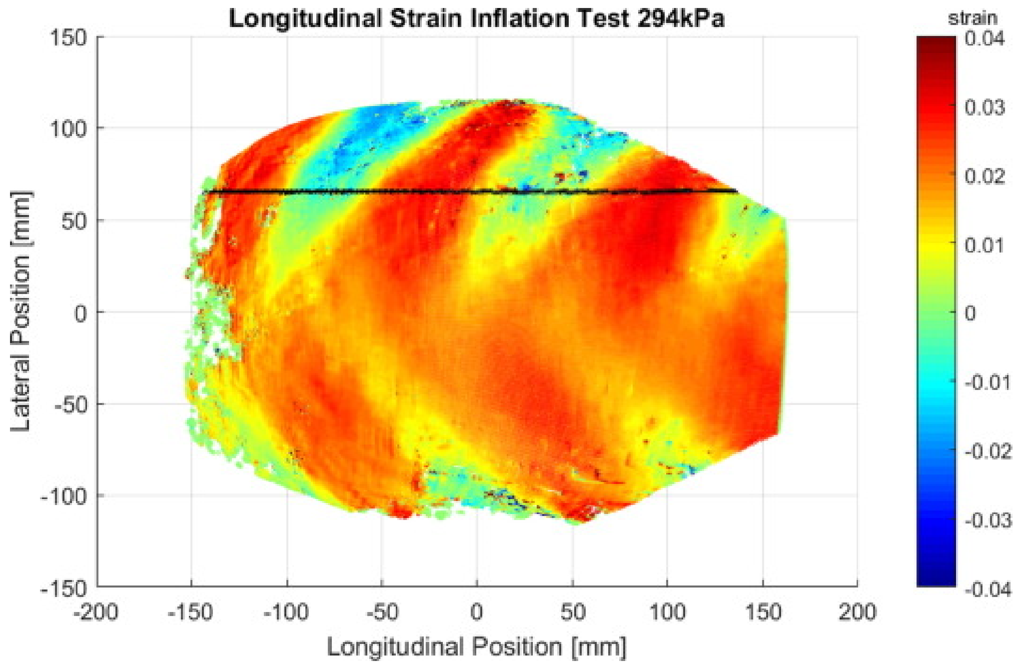

Fig. 4. Longitudinal Strain in During Inflation Test.

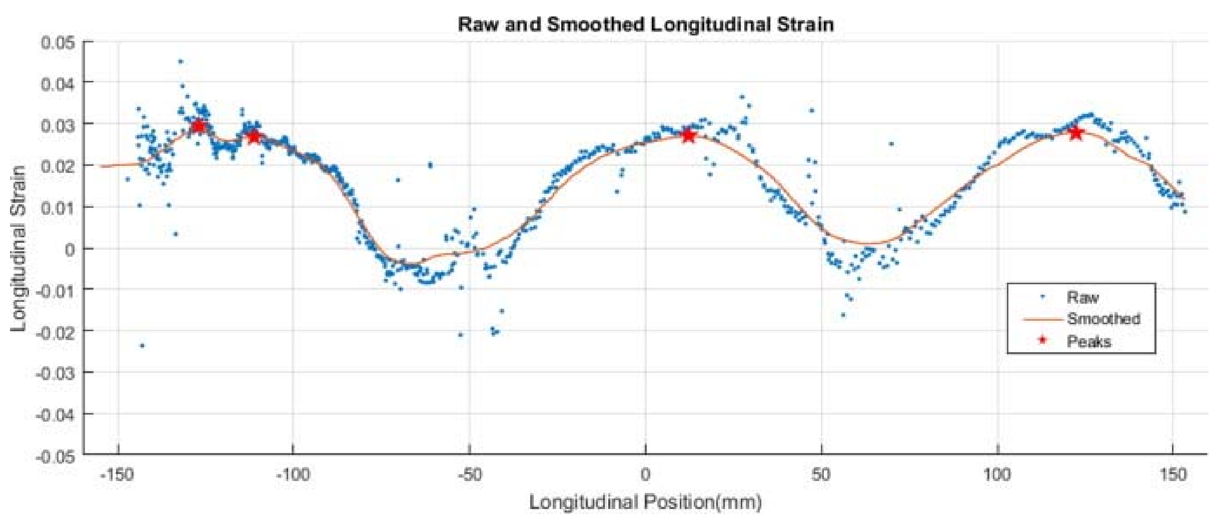

Fig. 5. Raw and Smoothed Longitudinal Strain Points in 64 mm to 66 mm Lateral Position Region.

3.2. Vertical loading test

Fig. 6 shows the image from one of the stereo cameras overlaid over the point-cloud with the approximate location of the tread blocks, shown in red Fig. 6(a). The position of the tread blocks was obtained from visually inspecting the tyre beforehand. The strain of the tyre was determined relative to an inflated tyre with no applied vertical load. Fig. 6 (b-d) shows the longitudinal strain of the tyre at the different tyre inflation pressures at similar vertical loads of approximately 7.3 kN.

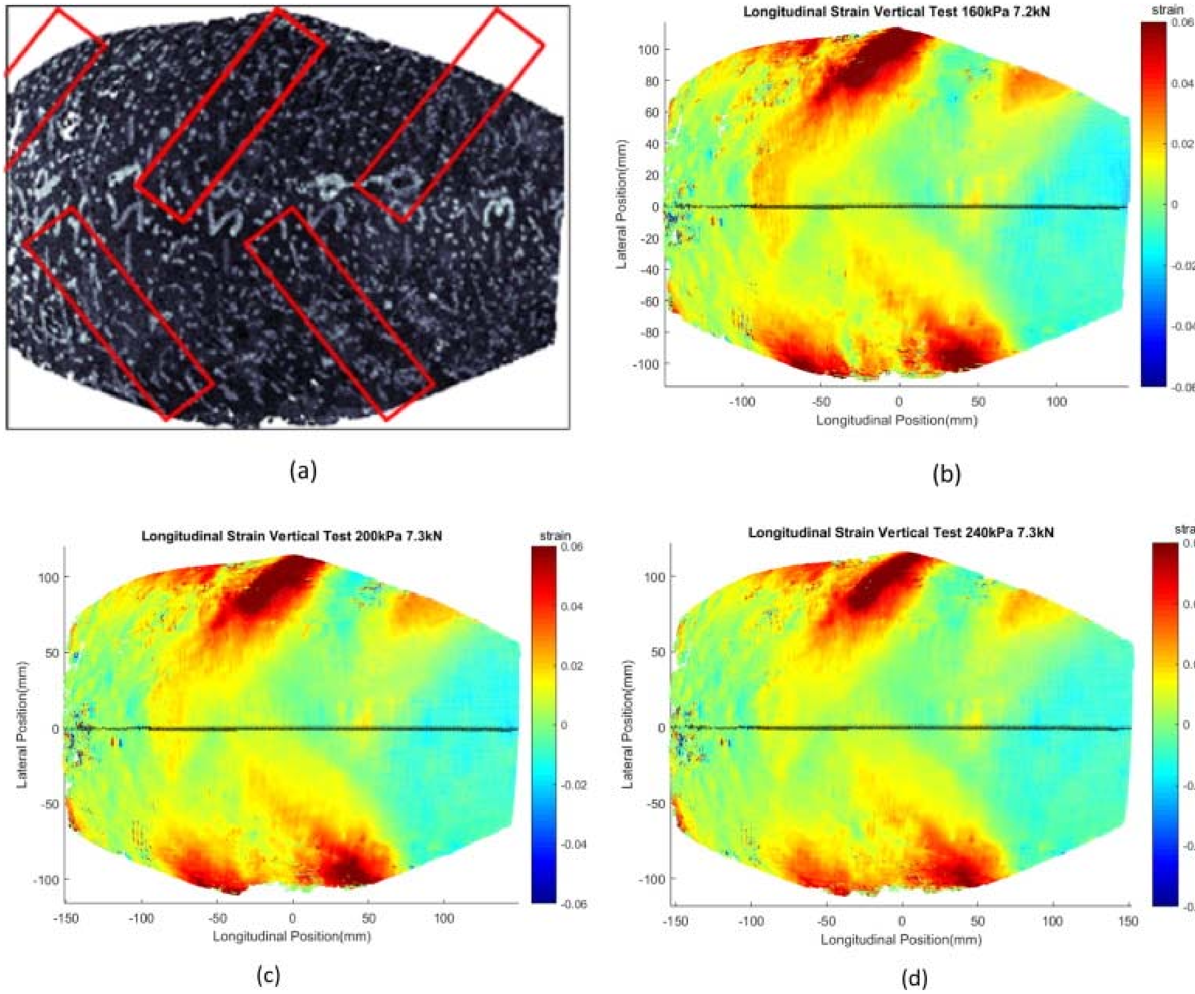

Fig. 6. (a) Tyre lugs overlaid on image of the inside of tyre, (b) Longitudinal strain at 160 kPa inflation pressure and 7.25 kN vertical load, (c) Longitudinal strain at 200 kPa inflation pressure and 7.35 kN vertical load, (d) Longitudinal strain at 240 kPa inflation pressure and 7.35 kN vertical load.

The three contact patches, Fig. 6 (b-d), show similar results. There are large longitudinal strains near the tread blocks close to the sidewalls. The middle region of the contact patch shows higher strain at lower inflation pressure. A longitudinal section through the middle of the contact patch, shown as a black line, is used to better illustrate the different longitudinal strain at different inflation pressures. The longitudinal section at each inflation pressure is shown in Fig. 7. At 160 kPa the longitudinal strain in the middle line of the contact patch peaks at 0.0195 (1.95%), at 200kPathe strain peaks at 0.0149 (1.49%) and at 240 kPa the strain peaks at 0.0107 (1.07%). The location of peak strain is constant at each tyre inflation pressure and is therefore a suitable position on the tyre to place a single point strain measurement, such as strain gauges, on the inner surface of the tyre. Using the strain measurement at this location it would be possible to measure the tyre inflation pressure if the vertical force is known. The sections also show that there are regions which show very little to no change in strain between tyre inflation pressures.

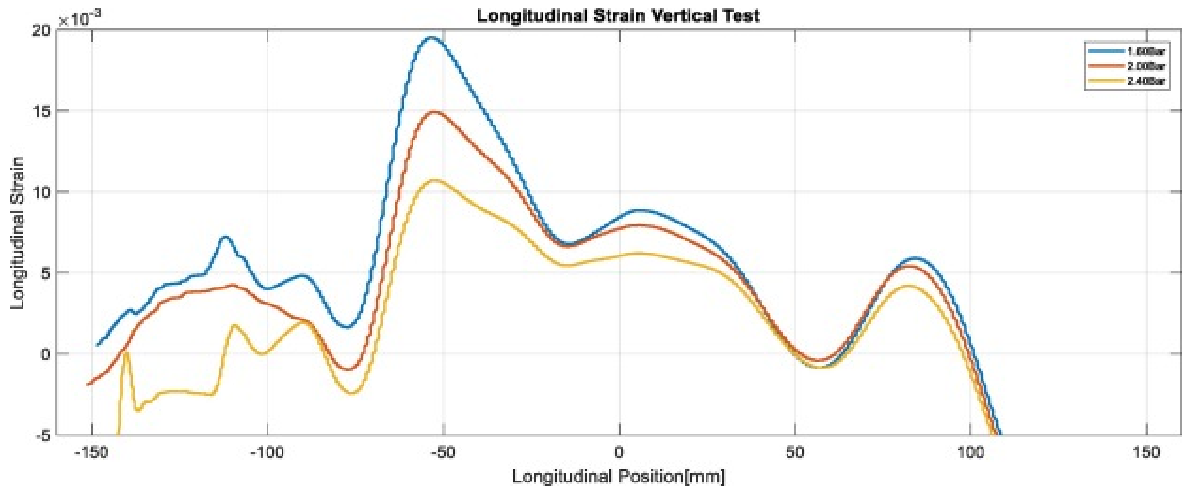

Fig. 7. Longitudinal strain for different tyre inflation pressures at 7.3 kN vertical force.

The effect of an increase in vertical force on the longitudinal strain is determined by taking a section through the full-field strain profile at different vertical loads. As shown in Fig. 6 (b-d), the strain is larger at the edges of the contact patch and therefore a section closer to the edge of the tyre would show more sensitivity to a change in applied vertical load. Therefore, a section at the 75 mm lateral position as shown in Fig. 8 (a) by the black line, is used. Fig. 8 (b) shows the sections at different vertical loads for an inflation pressure of 200 kPa. The figure clearly shows that the strain increases as the vertical force increases. It is also evident that there are regions in the contact patch which exhibit large strain changes and other regions with very small changes. This shows that there are more ideal positions to place single point strain measurements to measure the tyre force. It is also observed from Fig. 8(b) that the position at which the maximum strain is measured slightly shifts longitudinally. Therefore, to obtain a relationship between the longitudinal strain and applied vertical the maximum strain, as well as, a specific location on the tyre is used. The 0 mm longitudinal position is used as the fixed position as this location shows a high sensitivity to a change in applied vertical load. The relationship between strain, at 0 mm and the maximum, and force is depicted in Fig. 9. The raw data points, vertical load a longitudinal strain, are shown on the figure as markers. The figure also shows the strain at the 0 mm longitudinal position for tyre inflation pressures of 160 kPa and 240 kPa. A linear regression is also performed on all the raw data points and shown in the figure. The relationship at all tyre inflation pressures show a near linear correlation, between the strain and the applied vertical load, with the lowest R^2 value being 0.98 for all regressions. The gradient at all tyre inflation pressures are also similar which suggests that strain near the sidewall is not significantly affected by tyre inflation pressure.

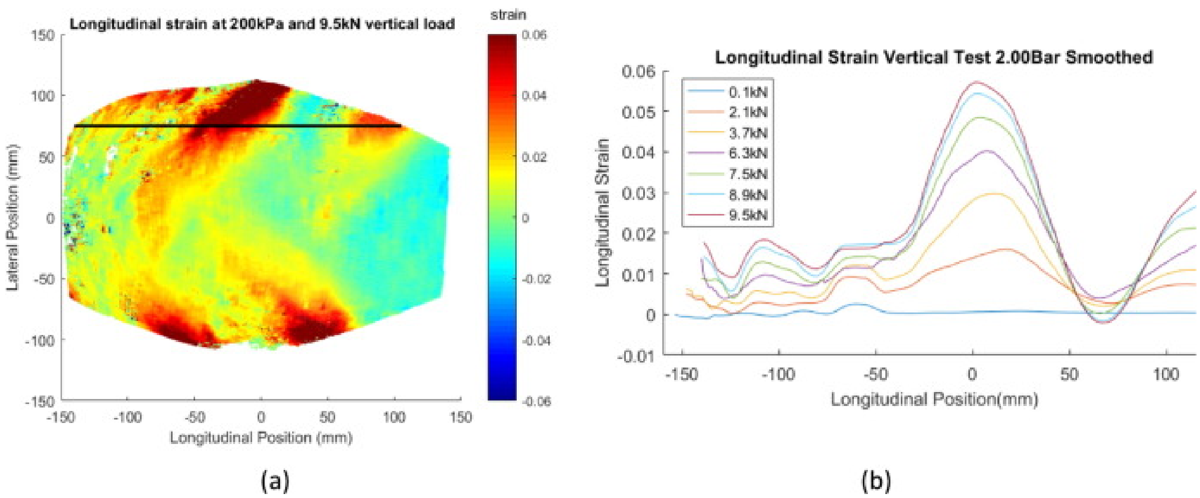

Fig. 8. a) Longitudinal strain of the tyre during vertical test at 200 kPa and vertical load equal to load index b) longitudinal sections at 75 mm laterally at different tyre loads.

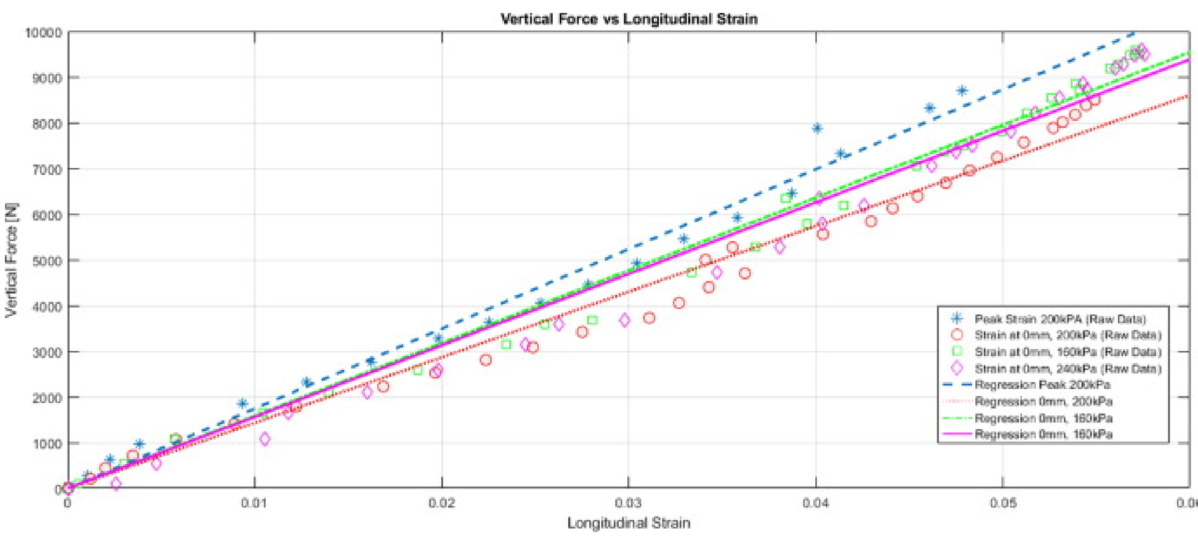

Fig. 9. Longitudinal Strain vs Vertical Force at different tyre inflation pressures with regression line for each tyre inflation pressure.

3.3. Longitudinal load test

Of interest in this test is the longitudinal strain in the tyre as the longitudinal load increases. It was found that the longitudinal strain is dominated primarily by the strain caused by the vertical force. Therefore, the reference state for the strain measurement is taken as a vertically loaded and longitudinally un-loaded state. This determines the increase in the longitudinal strain as a function of the longitudinally applied force and thus the effect of the vertical force is removed. Initial tests are first conducted at an inflation pressure of 160 kPa. This inflation pressure is chosen because at 160 kPa the tyre is less stiff in the longitudinal direction than at 200 kPa or 240 kPa. A vertical load of 6.3kN was applied to the tyre, before longitudinally loaded, which is 75% of the load index at 160 kPa. At higher loads the deflection from both longitudinal and vertical force resulted in too much deformation that lighting was significantly affected and resulted in poor measurement from T2Cam. The longitudinal strain for the contact patch is shown at the friction limits for the tyre, as it is displaced in both direction in Fig. 10. The longitudinal force produced in both direction are approximately 1.8kN before the tyre starts to slip.

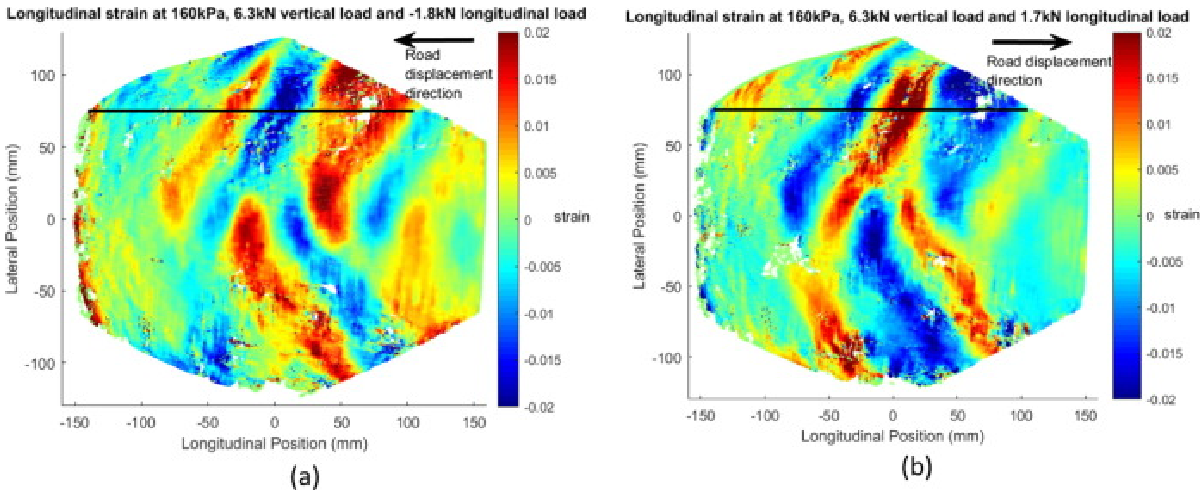

Fig. 10. a) Longitudinal strain vs vertical force for tyre fully deflected to the left. b) Longitudinal strain vs vertical force for tyre fully deflected to the right.

The figure shows that there are high strain values near the leading and trailing edges of the tread block. When the tyre is displaced the relatively stiff tread block rolls, pushing it into the contact patch region on one edge and pulling away from the contact patch region on the other. In the region where the tread block pushes into the contact patch region there is positive strain as rubber near the tread block edge is stretched apart with respect to the reference state. Conversely on the edge where the tread block pulls away from the contact patch the rubber is compressed to create negative strain. Regions that experience large positive longitudinal strain experience large negative strain when displaced in the opposite direction. Fig. 11 (a) shows the longitudinal strain of a longitudinal sections taken at 75 mm laterally (marked in black in Fig. 10 (a) and (b)) at the friction limits for both displacement directions of the tyre. The centre of the tread block which lies at about 0 mm longitudinally experiences low longitudinal strain, relative to a vertically loaded tyre, and almost no change when the direction of the displacement is changed. At negative displacement the largest compressive (negative) longitudinal strain is about $-0.013(-1.3\%)$. For the positive displacement, the largest tensile (positive) longitudinal strain is about $0.017(1.7\%)$. The difference in the change in longitudinal strain may be due to the tyre pattern is not being symmetrical in the longitudinal direction, which may result in the tyre deforming differently when loaded in different longitudinal directions. The sections at the negative and positive displacement extremes do appear to be near reflections of each other. The locations with large changes in strain could serve as suitable locations to measure strain while regions, which show almost no sensitivity, are ill suited to measure changes in applied longitudinal load. A longitudinal force vs longitudinal strain relationship is created and displayed in Fig. 11 (b). The point used to generate this relationship was taken at the 20 mm longitudinal position of the longitudinal section. The longitudinal section was taken at 75 mm laterally on the tyre, therefore, the location is (20, 75)mm (longitudinal and lateral) corresponds to a very sensitive region in applied longitudinal load. The obtained relationship is very linear, with in nature showing that the strain increases linearly at this location from the vertically loaded state. The effect of the tyre inflation pressure and vertical load on this relationship still needs to be determined.

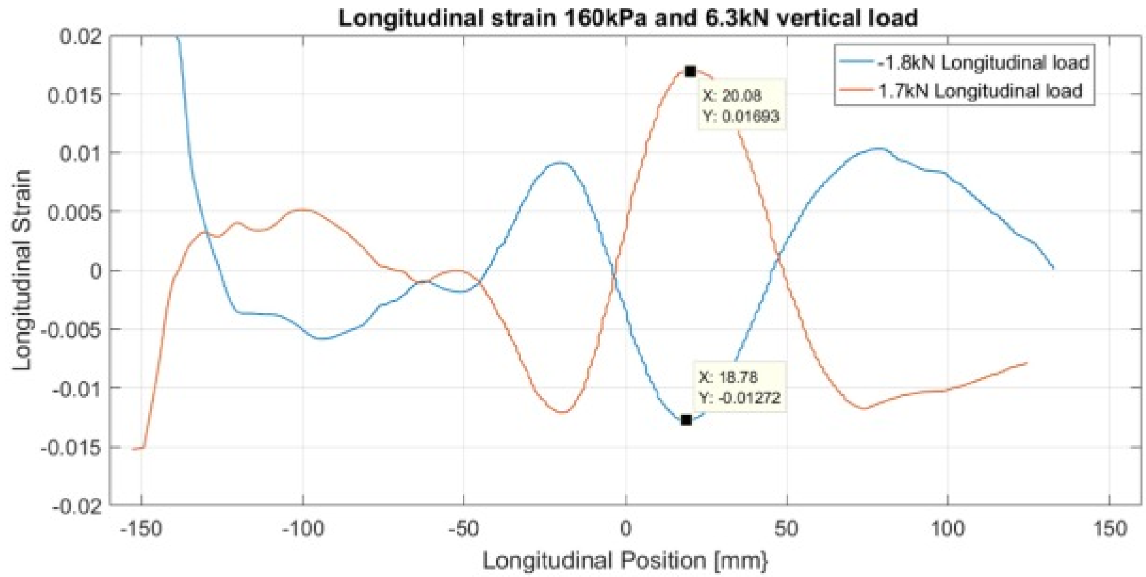

(a)

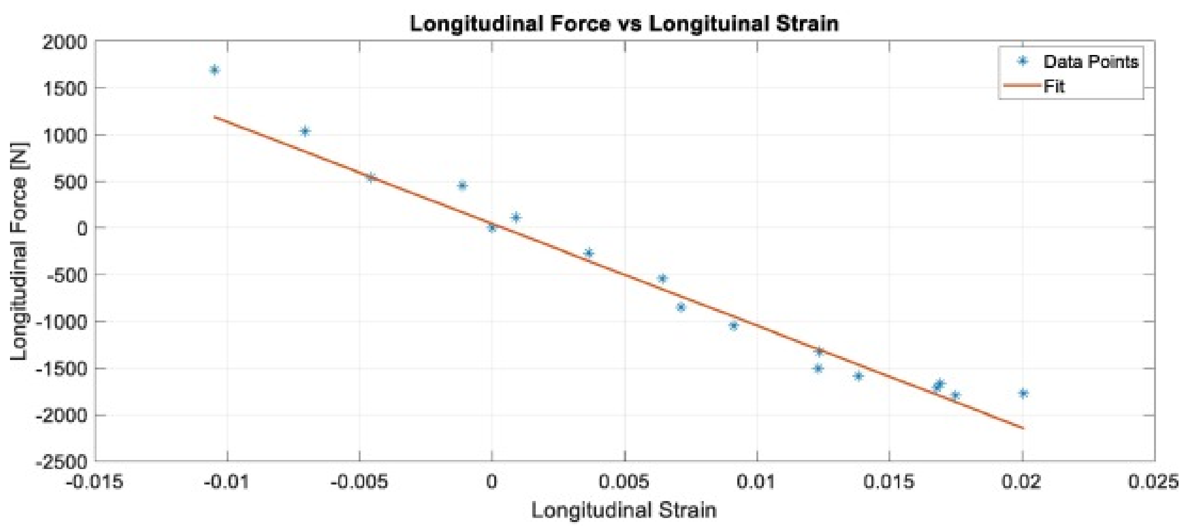

(b)

Fig. 11. a) Longitudinal strain for sections taken at 75 mm laterally for fully deflected tyre to the left and tight. b) Longitudinal force vs longitudinal strain for point (20,75) mm on the tyre.

4. Conclusion

This study set out to determine firstly whether the lugs of an agricultural tyre significantly affect the strain produced on the inside of the tyre. Secondly whether there are relationships between the applied loads and strain produced inside a tyre which could be used for force estimation. This study was conducted in quasi-static conditions It was found that the strain profile of the tyre is non-homogeneous in nature and is significantly affected by the tyre lugs.

The pattern of the lugs could clearly be observed in the measurements of the strain fields. An inflation test showed that the regions where the lugs are located significantly changes the stiffness of the tyre. The increase in stiffness resulted in the tyre lugs being visible on the longitudinal strain on the inside of the tyre during tyre inflation. During vertical loading the tyre strain profile was found to be non-homogeneous with areas that have very high strain sensitivity and regions which remain largely unstrained. This indicates that position where a single point strain measurement is made should be considered to ensure that adequate sensitivity to applied loads are obtained. A relationship between the vertical load and longitudinal strain of the tyre was developed. This relationship was obtained at three different inflation pressures. Results show that the relationship between vertical load and longitudinal strain is largely unaffected by inflation pressure in regions close to the tyre sidewall. During the longitudinally loaded test it was found that the strain measurements are dominated by the vertical loading. The strain was therefore determined relative to the vertical loaded tyre and showed that a linear relationship between the longitudinal strain and applied longitudinal load exists. The effects of tyre pressure and vertical load on the results still need to be investigated. Overall the method provides better insight in the strain patterns induced on the inside of a large lugged tyre compared to single point strain measurements as the strain is determined for the entire contact patch using one sensor. The results from the study shows that relationship between applied loads on the tyre and the induced strain of the tyre exists for large lugged tyres. These relationships could be further developed in order for strain measurements to be used to determine the loads applied to the tyre. The measurement method may be very beneficial in aiding in the development of future smart tyres on large lugged tyres. Future work will be performed with dynamic tests and in soft soil to better understand the strain produced in conditions where an agricultural tyre will operate.

Declaration of Competing Interest

The authors declare that they have no known competing financial interests or personal relationships that could have appeared to influence the work reported in this paper.

References

Baker, S., Mattews, I., 2004. Lucas-Kanade 20 years on: a unifying framework. Int. J.Comput. Vis. 56, 221–255.

Botha, T.R., Guthrie, A.G., Jiminez, E., Els, P.S., Sandu, C., 2017, Tyre LongitudinalVelocity and Slip Measurements from the Inside of a Tyre. 19th International &14th European-African Regional Conference of the ISTVS, 25.-27.09.2017Budapest. In: Proceedings of the 19th International & 14th European-AfricanRegional Conference of the ISTVS, S.1–10.

Braghin, F., Brusarosco, M., Cheli, F., Cigada, A., Manzoni, S., Mancosu, F., 2006.Measurement of contact forces and patch features by means of accelerometersfixed inside the tire to improve future car active control. Veh. Syst. Dynam. 44(sup1), 3–13.

Fan, Q., Qin, Z., Gao, S., Wu, Y., Pionteck, J., Mäder, E., Zhu, M. The use of a carbonnanotube layer on apolyurethane multifilament substrate for monitoringstrains as large as 400%.Carbon. 2012, 50, 4085–4092.

Feldesi, F., Botha, T.R., Els, P.S., 2018. Improvement Of 3d Contact PatchMeasurement Using Cameras Inside Rolling Tyres. 10th Asia-Pacific RegionalConference in Kyoto, Japan, July 11-13, 2018.

Garcia-Pozuelo, D., Olatunbosun, O., Yunta, J., Yang, X., Diaz, V., 2017. A novel strain-based method to estimate tire conditions using fuzzy logic for intelligent tires.Sensors 17 (2), 350.

Garcia-Pozuelo, D., Olatunbosun, O., Strano, S., Terzo, M., 2019. A real-time physicalmodel for strain-based intelligent tires. Sens. Actuat. A 288, 1–9.

Green, R.W., 2011. A Non-contact Method for Sensing Tire Contact PatchDeformation Using a Monocular Vision System and Speckled Image Tracking.Auburn University, Auburn.Guthrie, A.G., Botha, T.R., Els, P.S., 2017. 3D contact patch measurement insiderolling tyres. J. Terramech. 69, 13–21.

Hiroaka, N., Matsuzaki, R., Akira, T., 2009. Concurrent Monitoring of In-plane Strainand Out-of-plane Displacement of Tire Using Digital Image Correlation Method.J. Solid Mech. Mater. Eng. 3 (11), 1148–1159.

Hong, S., Erdogan, G., Hedrick, K., Borrelli, F., 2013. Tyre–road friction coefficientestimation based on tyre sensors and lateral tyre deflection: modelling,simulations and experiments. Veh. Syst. Dynam. 51 (5), 627–647.

Niskanen, A.J., Tuononen, A.J., 2014. Three 3-axis accelerometers fixed inside thetyre for studying contact patch deformations in wet conditions. Veh. Syst.Dynam. 52 (sup1), 287–298.

Ruggeri, M., Vecchiattini, A., 2018. New CTPE Sensors For Tire Monitoring. 10thAsia-Pacific Regional Conference in Kyoto, Japan, July 11-13, 2018.

Tuononen, A.J., 2008. Optical position detection to measure tyre carcass deflections.Veh. Syst. Dynam. 46 (6), 471–481.Tuononen, A.J., 2009. On-board estimation of dynamic tyre forces from opticallymeasured tyre carcass deflections. Int. J. Heavy Veh. Syst. 16 (3), 362–378.

Tuononen, A.J., 2011. Laser triangulation to measure the carcass deflections of arolling tire. Measur. Sci. Technol. 22 (12), 125304.

Xiong, Y., Tuononen, A.J., 2015. The in-plane deformation of a tire carcass: analysisand measurement. Case Stud. Mech. Syst. Signal Process. 2, 12–18.